Mechanics of Materials 50 (2012) 88–99

Contents lists available at SciVerse ScienceDirect

Mechanics of Materials

journal homepage: www.elsevier.com/locate/mechmat

Optimization of magnetoelectricity in multiferroic fibrous composites

Hsin-Yi Kuo *, Yong-Liang Wang

Department of Civil Engineering, National Chiao Tung University, Hsinchu 30010, Taiwan

ARTICLE INFO

Article history:
Received 29 August 2011
Received in revised form 10 January 2012
Available online 24 March 2012

Keywords:
Magnetoelectricity
Fibrous composites
Crystallographic orientation
Mori–Tanaka's method
Finite element analysis
Optimization

ABSTRACT

We propose a method to optimize the effective magnetoelectric voltage coefficient of fibrous composites made of piezoelectric and piezomagnetic phases. The optimization of magnetoelectricity is with respect to the crystallographic orientations and the volume fraction for the two materials. We show that the effective in-plane ($\alpha^*_{E,11}$) and out-of-plane ($\alpha^*_{E,33}$) coupling constants can be enhanced many-fold at the optimal orientation compared to those at normal orientation. For example, we show that the constants are 101 and 5 times larger for the optimal orientation of $CoFe_2O_4$ fibers in a $BaTiO_3$ matrix of the optimized volume fraction compared to the normal orientation, while they are 43 and 5 times larger for $BaTiO_3$ fibers in a $CoFe_2O_4$ matrix. The predictions are in good agreement with the finite element analysis.

1. Introduction

Magnetoelectric (ME) materials, which show a polarization induced by an applied magnetic field, or conversely, a magnetization induced by an applied electric field, have been the focus of recent research due to their coupling between the electric and magnetic fields. This make them particularly appealing and promising for a wide range of applications, such as ME data storage and switching, magnetic field detectors, and amplification and frequency conversion between the electric and magnetic fields (Fiebig, 2005). However, the ME effect in single phase materials is rather weak or cannot be observed at room temperature (Astrov, 1960; Rado and Folen, 1961). Composite materials, on the other hand, offer an alternative option for improvement of the ME coupling, as explained in recent reviews by Eerenstein et al. (2006) and Nan et al. (2008). This much stronger ME effect could be realized in a composite made of piezoelectric and piezomagnetic/magnetostrictive phases using product properties: an applied magnetic field creates a strain in the piezomagnetic/magnetostrictive material which in turn creates a strain in the piezoelectric material, resulting in an electric polarization.

A variety of models have been proposed to predict the effective magnetoelectroelastic moduli of the multiferroic composite. The estimates of the effective properties of ME composites are usually obtained by various approximate mean-field models (Nan, 1994; Benveniste, 1995; Wu and Huang, 2000). The exact solutions for local fields are available for simple microstructures such as a single ellipsoidal inclusions (Huang and Kuo, 1997; Li and Dunn, 1998a), periodic arrays of circular/elliptic fibrous ME composites (Kuo, 2011; Kuo and Pan, 2011) and laminates (Srinivas et al., 2001; Bichurin et al., 2003), etc. A homogenization method was employed for calculating the effective properties of periodic ME fibrous composites (Aboudi, 2001; Camacho-Montes et al., 2009), while numerical methods based on the finite element analysis have also been developed to address ME composites with more general microstructures (Liu et al., 2004; Lee et al., 2005). However, much of this theoretical development limits itself to the situation where the poling direction (magnetic axis) of the piezoelectric (piezomagnetic) material is either normal to or along the layer (fiber) direction. Further, many of these works assume transverse isotropy or uniaxial symmetry.

In the work of Li and Dunn (1998b), they used Eshelby's pioneering approach to study the fields in and around inclusions and inhomogeneities in *anisotropic* solids exhibiting

* Corresponding author.
E-mail address: hykuo@mail.nctu.edu.tw (H.-Y. Kuo).

0167-6636/$ - see front matter © 2012 Elsevier Ltd. All rights reserved.
http://dx.doi.org/10.1016/j.mechmat.2012.03.005

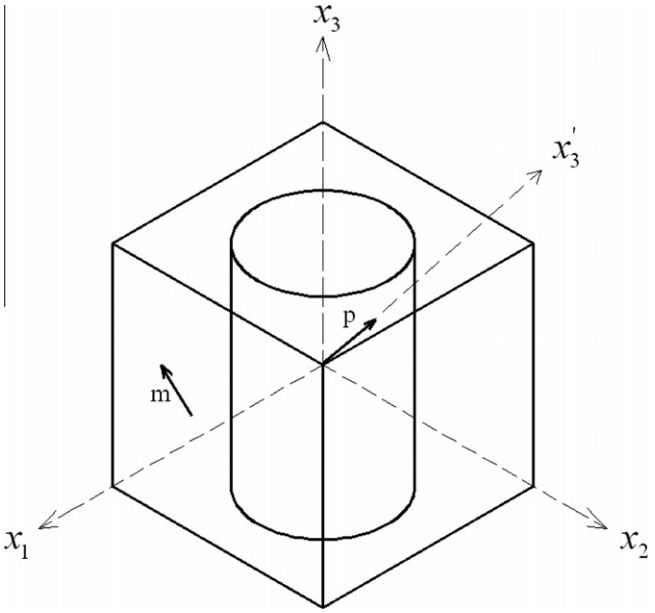

Fig. 1. The fibrous composite configurations.

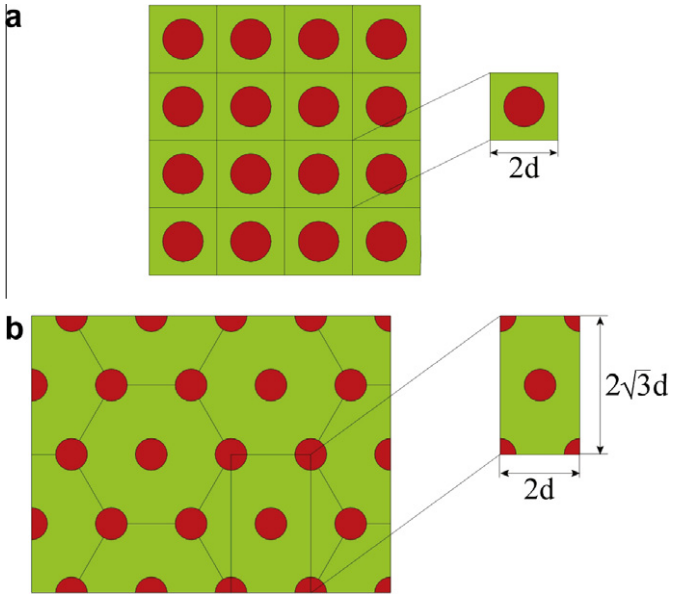

Fig. 2. A schematic representation of a unit cell. (a) A square array. (b) A hexagonal array.

full coupled-field behavior. Later, Li (2000a) developed a numerical algorithm to evaluate the magnetoelectroelastic Eshelby's tensor for the general material symmetry and ellipsoidal inclusion shape. Recently, experiments by Yang et al. (2006) and Wang et al. (2008) showed that single crystals are attractive and the effective ME coefficient of the laminate can depend sensitively on the crystallographic orientation of the material. Srinivas et al. (2006) developed a mean-field Mori–Tanaka model to calculate the ME coupling of matrix-based multiferroic composites, emphasing the effects of shape and orientation distribution of second phase particles. In addition, Kuo et al. (2010) proposed a simple framework to optimize the effective magnetoelectric response of a piezoelectric-magnetostrictive bilayer. The essence of the concept is that the induced electric field in the piezoelectric phase could be increased if the *orientation* and *volume fraction* of the piezoelectric layer can be carefully chosen. They have used it to show that, for anisotropic materials as in single crystals, the optimal ME response is obtained for non-trivial orientations.

Table 1
Material parameters of $BaTiO_3$ and $CoFe_2O_4$ (Li and Dunn, 1998a).

Property	$BaTiO_3$	$CoFe_2O_4$
C_{11} (GPa)	166	286
C_{12} (GPa)	77	173
C_{13} (GPa)	78	170
C_{33} (GPa)	162	269.5
C_{44} (GPa)	43	45.3
e_{15} (C/m^2)	11.6	0
e_{31} (C/m^2)	-4.4	0
e_{33} (C/m^2)	18.6	0
q_{15} (N/Am)	0	550
q_{31} (N/Am)	0	580.3
q_{33} (N/Am)	0	699.7
κ_{11} (nC^2/Nm^2)	11.2	0.08
κ_{33} (nC^2/Nm^2)	12.6	0.093
μ_{11} ($\mu Ns^2/C^2$)	5	590
μ_{33} ($\mu Ns^2/C^2$)	10	157

Motivated by these advances, in this paper we optimize the effective ME voltage coefficient of a multiferroic fibrous composite without any assumptions on the symmetry of the underlying materials and without any assumptions on the crystallographic orientations of the materials. We give the basic equations and Euler transformations regarding the magnetoelectroelasticity in Section 2.1. In Section 2.2, we derive a micromechanical model for the multiferroic composites. We introduce the finite element analysis in Section 2.3, which is used for comparison with the micromechanical approach. This methodology is illustrated in Section 3 using composites of cobalt ferrite ($CoFe_2O_4$) and barium titanate ($BaTiO_3$). We show that the optimal orientations can be non-trivial and the enhancement to be many-fold over the normal orientations.

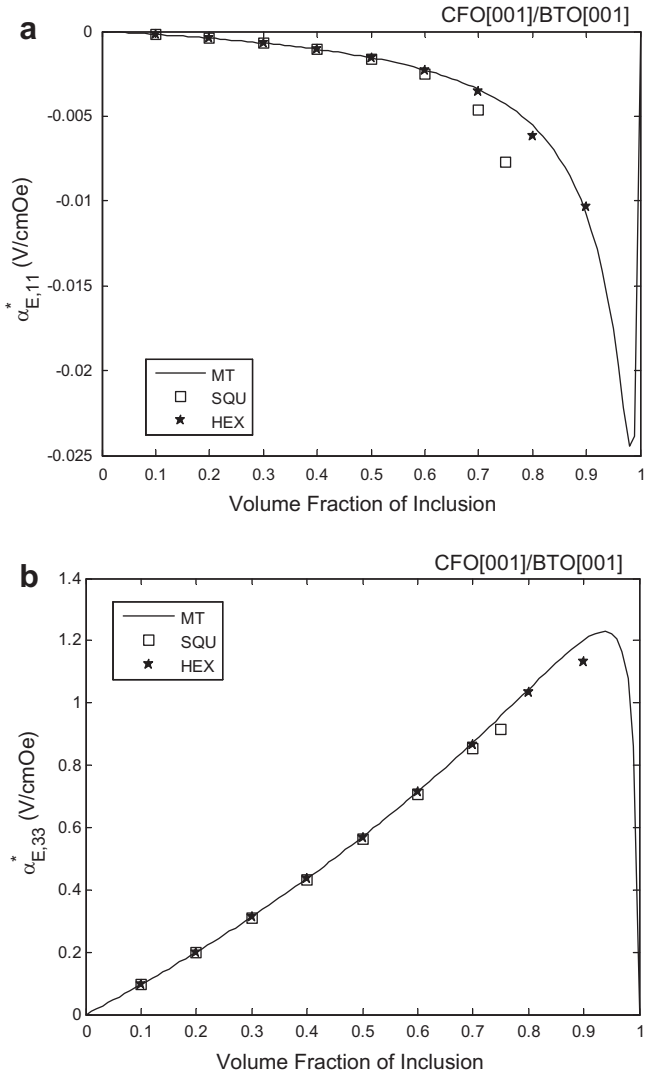

Fig. 3. The ME voltage coefficients of the CFO fibers in a BTO matrix at the normal direction versus the fiber volume fraction. (a) In-plane ME voltage coefficient $\alpha^*_{E,11}$. (b) Out-of-plane ME voltage coefficient $\alpha^*_{E,33}$.

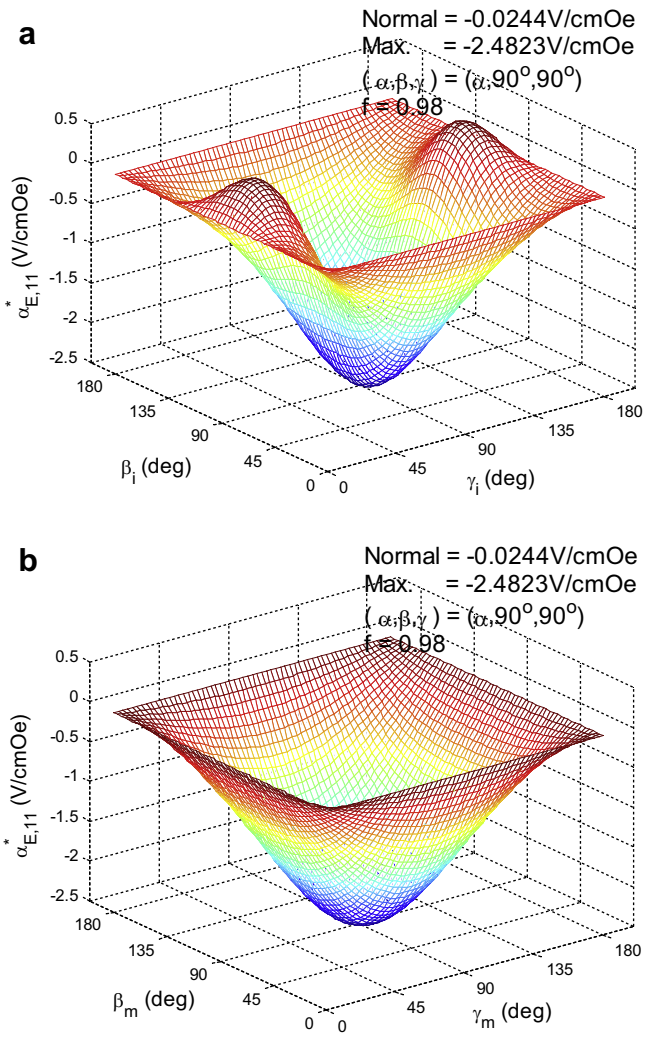

Fig. 4. The in-plane ME voltage coefficient of the CFO fibers in a BTO matrix for various orientations of CFO and BTO. The subscripts i and m denote the inclusion and matrix, respectively. Note that this coefficient depends only on the Euler angles β and γ and is independent of α. The optimized constant occurs at both phases poled along the same direction.

2. Model

2.1. Basic equations

Consider a perfectly bonded magnetoelectric circular fibrous composite made of piezoelectric and piezomagnetic materials as shown in Fig. 1. The response of the composite in a Cartesian frame with the x_3 direction normal to the plane can be described by the following general equations (Alshits et al., 1992)

$$\begin{aligned} \sigma_{ij} &= C_{ijkl}\varepsilon_{kl} - e_{lij}E_l - q_{lij}H_l, \\ D_i &= e_{ikl}\varepsilon_{kl} + \kappa_{il}E_l + \lambda_{li}H_l, \\ B_i &= q_{ikl}\varepsilon_{kl} + \lambda_{il}E_l + \mu_{il}H_l, \end{aligned} \tag{1}$$

where σ_{ij} and ε_{ij} are the stress and strain; D_i and E_i are the electric displacement and electric field vectors; B_i and H_i are the magnetic flux and magnetic field vectors; C_{ijkl} is the elastic stiffness (fourth-order tensor), e_{ijk} is the piezoelectric moduli (third-order), q_{ijk} is the piezomagnetic moduli (third-order), κ_{ij} is the permittivity (second-order), μ_{ij} is the permeability (second-order) and λ_{ij} is the magnetoelectric coefficient (second-order). The summation convention is used. The symmetry conditions satisfied by the moduli are given by Nye (1985).

The strain ε_{ij}, electric field E_i, and magnetic field H_i are respectively defined by the displacement u_i, electric potential φ, and magnetic potential ψ via

$$\varepsilon_{ij} = \frac{1}{2}\left(u_{i,j} + u_{j,i}\right), \quad E_i = -\varphi_{,i}, \quad H_i = -\psi_{,i}. \tag{2}$$

Here the comma in the subscript denotes partial derivative.

To obtain the effective properties of this medium, we need to solve for equilibrium equations

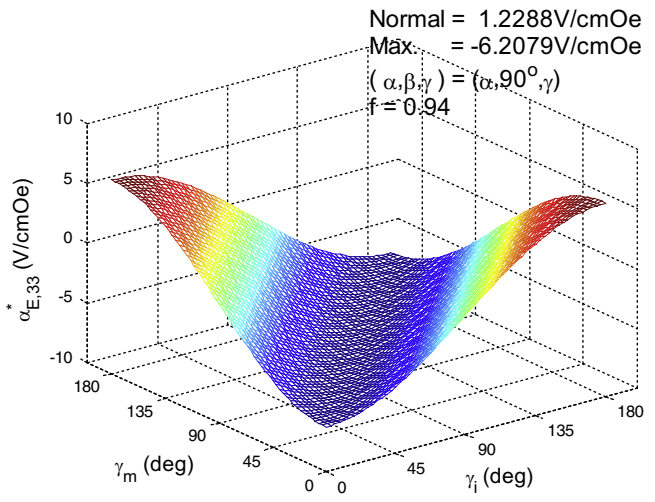

Fig. 5. The out-of-plane ME voltage coefficient of the CFO fibers in a BTO matrix for various orientations of CFO and BTO. The subscripts i and m denote the inclusion and matrix, respectively. Note that this coefficient depends only on the Euler angles β and γ and is independent of α. The optimized constant occurs at both phases poled along the same direction.

$$\sigma_{ij,i} = 0, \quad D_{i,i} = 0, \quad B_{i,i} = 0, \tag{3}$$

along with the analogous interfacial conditions and appropriate boundary conditions.

The constitutive laws, strain-displacement and equilibrium equations can be rewritten in a more concise form as follows (Alshits et al., 1992)

$$\Sigma_{iJ} = L_{ijMn} Z_{Mn}, \quad Z_{Mn} = U_{M,n}, \quad \Sigma_{iJ,i} = 0, \tag{4}$$

where

$$\Sigma_{iJ} = \begin{cases} \sigma_{ij}, & J = 1,2,3, \\ D_i, & J = 4, \\ B_i, & J = 5, \end{cases} \qquad Z_{Mn} = \begin{cases} \varepsilon_{mn}, & M = 1,2,3, \\ -E_n, & M = 4, \\ -H_n, & M = 5, \end{cases}$$

$$U_M = \begin{cases} u_m, & M = 1,2,3, \\ \varphi, & M = 4, \\ \psi, & M = 5. \end{cases} \tag{5}$$

The magnetoelectroelastic moduli are expressed as

$$L_{ijMn} = \begin{cases} C_{ijmn}, & J,M = 1,2,3, \\ e_{ijn}, & M = 4,\ J = 1,2,3, \\ q_{ijn}, & M = 5,\ J = 1,2,3, \\ e_{imn}, & J = 4,\ M = 1,2,3, \\ -\kappa_{in}, & J = 4,\ M = 4, \\ -\lambda_{in}, & J = 4,\ M = 5, \\ q_{imn}, & J = 5,\ M = 1,2,3, \\ -\lambda_{in}, & J = 5,\ M = 4, \\ -\mu_{in}, & J = 5,\ M = 5, \end{cases} \tag{6}$$

where the upper case subscript ranges from 1 to 5 and the lower case subscript ranges from 1 to 3. Repeated upper case subscripts are summed from 1 to 5.

The equations above refer the material properties to the fiber frame (Fig. 1). However, the material properties are commonly described in the crystallographic frame and we need to transform them to the fiber frame. To this end, let us denote the crystal frame with primes and introduce the rotation matrix a_{ij}. This is given in terms of the three Euler angles (α, β, γ) as follows (Arfken and Weber, 2001)

$$\begin{pmatrix} a_{11} & a_{12} & a_{13} \\ a_{21} & a_{22} & a_{23} \\ a_{31} & a_{32} & a_{33} \end{pmatrix} = \begin{pmatrix} \cos\gamma\cos\beta\cos\alpha - \sin\gamma\sin\alpha & \cos\gamma\cos\beta\sin\alpha + \sin\gamma\cos\alpha & -\cos\gamma\sin\beta \\ -\sin\gamma\cos\beta\cos\alpha - \cos\gamma\sin\alpha & -\sin\gamma\cos\beta\sin\alpha + \cos\gamma\cos\alpha & \sin\gamma\sin\beta \\ \sin\beta\cos\alpha & \sin\beta\sin\alpha & \cos\beta \end{pmatrix}. \tag{7}$$

For the change of frame, the material parameters then follow the tensor transformation rules for second-, third- and fourth-order tensors

$$\begin{aligned} \kappa_{ij} &= a_{im} a_{jn} \kappa'_{mn}, \\ \mu_{ij} &= a_{im} a_{jn} \mu'_{mn}, \\ e_{ijk} &= a_{im} a_{jn} a_{ko} e'_{mno}, \\ q_{ijk} &= a_{im} a_{jn} a_{ko} q'_{mno}, \\ C_{ijkl} &= a_{im} a_{jn} a_{ko} a_{lp} C'_{mnop}, \end{aligned} \tag{8}$$

where the primed quantities $\left(\kappa'_{ij}, \mu'_{ij}, e'_{ijk}, q'_{ijk}, C'_{ijkl}\right)$ denote the material properties referred to the crystallographic frame.

2.2. Effective moduli and Mori–Tanaka's approach

We are interested in the effective behavior for a situation where we have a large number of inclusions. The effective material properties are defined in terms of average fields,

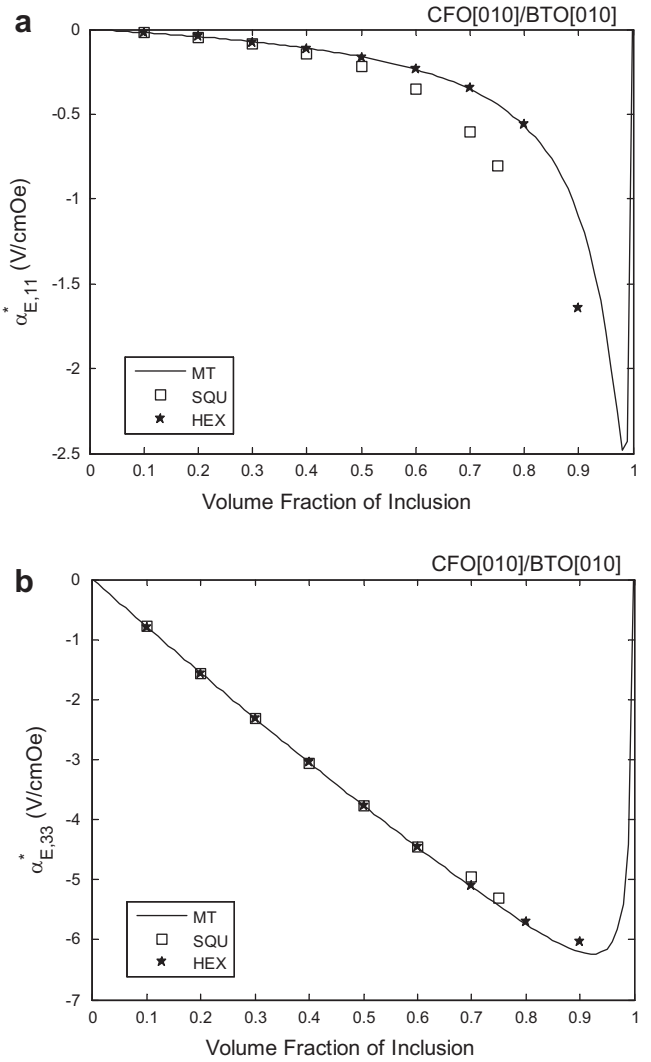

Fig. 6. The optimal ME voltage coefficients of the CFO fibers in a BTO matrix for various fiber volume fraction. (a) In-plane ME voltage coefficient $\alpha^*_{E,11}$. (b) Out-of-plane ME voltage coefficient $\alpha^*_{E,33}$.

$$\langle \Sigma_{ij} \rangle = L^*_{ijMn} \langle Z_{Mn} \rangle, \tag{9}$$

where the angular brackets denote the average over the representative volume element (unit cell in the case of periodic composites), and L^*_{ijMn} denotes the effective magnetoelectroelastic parameters of the composite. Due to the linearity, the generalized strain in the inclusion for a two-phase composite is (Srinivas et al., 2006)

$$Z_{Mn} = A_{MnAb} \langle Z_{Ab} \rangle, \tag{10}$$

where A_{MnAb} is the generalized strain concentration tensor of the inclusion. As a result, the effective moduli can be determined for a two-phase composite as

$$L^*_{ijAb} = L^{(m)}_{ijAb} + f\left(L^{(i)}_{ijMn} - L^{(m)}_{ijMn}\right) A_{MnAb}. \tag{11}$$

Here f is the volume fraction of the inclusion, and the superscripts m and i denote the matrix and inclusion, respectively.

The concentration tensor A_{MnAb} can be determined by the Mori–Tanaka's approach as

$$A_{MnAb} = A^{dil}_{MnJi}\left[(1-f) I_{JiAb} + f A^{dil}_{JiAb}\right]^{-1}, \tag{12}$$

with the dilute concentration tensor A^{dil}_{MnAb} given by

$$A^{dil}_{MnAb} = \left[I_{MnAb} + S_{MnLk}(L^{(m)}_{LkiJ})^{-1}\left(L^{(i)}_{ijAb} - L^{(m)}_{ijAb}\right)\right]^{-1}, \tag{13}$$

where S_{MnAb} is the magnetoelectroelastic Eshelby tensor, which is a function of the magnetoelectroelastic moduli of matrix, the shape and orientation of the inclusion, and is described by Li and Dunn (1998b).

$$S_{MnAb} = \frac{1}{8\pi} L_{ijAb} \begin{cases} \int_{-1}^{1}\int_{0}^{2\pi} \left[G_{mjin}(\mathbf{z}) + G_{njim}(\mathbf{z})\right] d\theta d\xi_3, & M = 1,2,3, \\ 2\int_{-1}^{1}\int_{0}^{2\pi} G_{4jin}(\mathbf{z}) d\theta d\xi_3, & M = 4, \\ 2\int_{-1}^{1}\int_{0}^{2\pi} G_{5jin}(\mathbf{z}) d\theta d\xi_3, & M = 5. \end{cases} \tag{14}$$

In the above equation, $z_i = \xi_i / a_i$ (no summation on i), a_i is the semi-axis of size and ξ_1 and ξ_2 can be expressed in

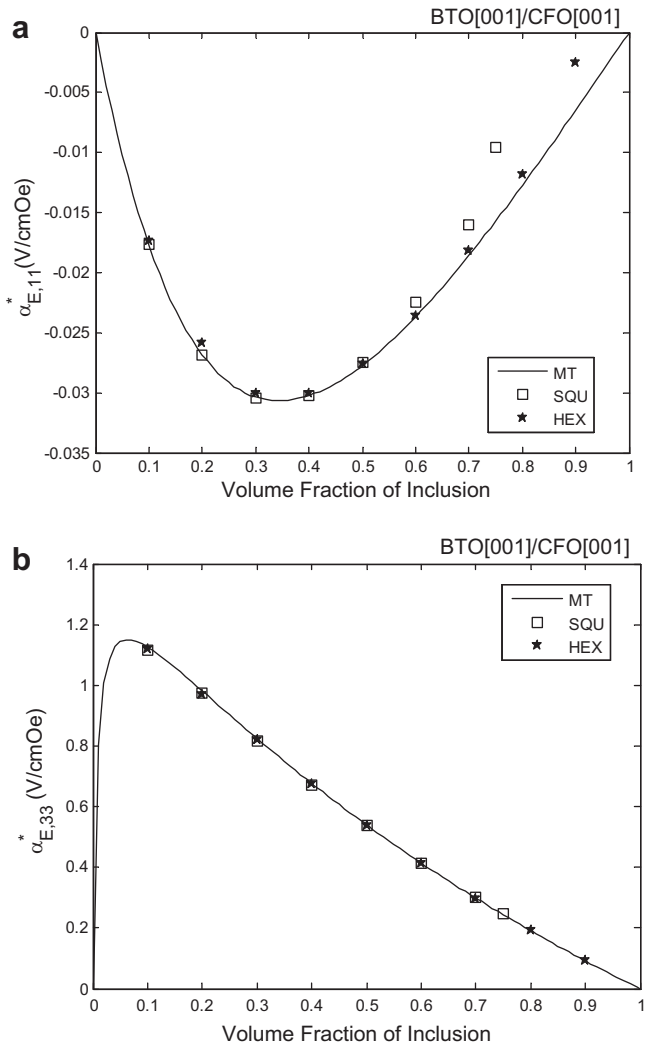

Fig. 7. The ME voltage coefficients of the BTO fibers in a CFO matrix at the normal direction versus the fiber volume fraction. (a) In-plane ME voltage coefficient $\alpha^*_{E,11}$. (b) Out-of-plane ME voltage coefficient $\alpha^*_{E,33}$.

terms of ξ_3 and θ by $\xi_1 = \sqrt{1-\xi_3^2}\cos\theta$ and $\xi_2 = \sqrt{1-\xi_3^2}\sin\theta$. In addition $G_{MJin} = z_i z_n K^{-1}_{MJ}(\mathbf{z})$, where K^{-1}_{MJ} is the inverse of $K_{JR} = z_i z_n L_{ijRn}$. Li and Dunn (1998a) have obtained the closed-form expressions of magneto-electroelastic Eshelby's tensors for the aligned elliptic cylinder inclusion in a transversely isotropic medium. However, for the piezoelectric and piezomagnetic materials with arbitrary poling direction and magnetic axes as discussed in this work, we resort to Gauss quadrature numerical method to calculate S_{MnAb}. The integral (14) then is approximated by the weighted sum of function values at certain integration points (Li, 2000a).

2.3. Finite element analysis

In this section we introduce the finite element analysis which is used for comparison with the Mori–Tanaka's approach. We first choose an appropriate representative volume element (RVE), a periodic unit cell, which captures the major features of the underlying microstructure. There are five possible ways of packing cylinders a regular array in two dimensions (See Kittel, 2005 for instance). Here we concentrate on the two lattices, rectangular and hexagonal arrays (Fig. 2).

Because of the periodicity in the composite structure, the displacement u_i, the electric potential φ and the magnetic potential ψ in any point of the unit cell can be expressed in terms of those at an equivalent point in another RVE such that the periodic boundary conditions

$$\begin{aligned} U_M(d,x_2,x_3) &= U_M(-d,x_2,x_3) + \langle U_{M,1}\rangle 2d,\\ U_M(x_1,d,x_3) &= U_M(x_1,-d,x_3) + \langle U_{M,2}\rangle 2d,\\ U_M(x_1,x_2,d) &= U_M(x_1,x_2,-d) + \langle U_{M,3}\rangle 2d, \end{aligned} \tag{15}$$

are satisfied for a square array. Here U_M is defined in (5) and $2d$ is the length of the unit cell. Similarly, the periodic boundary conditions for a hexagonal array are

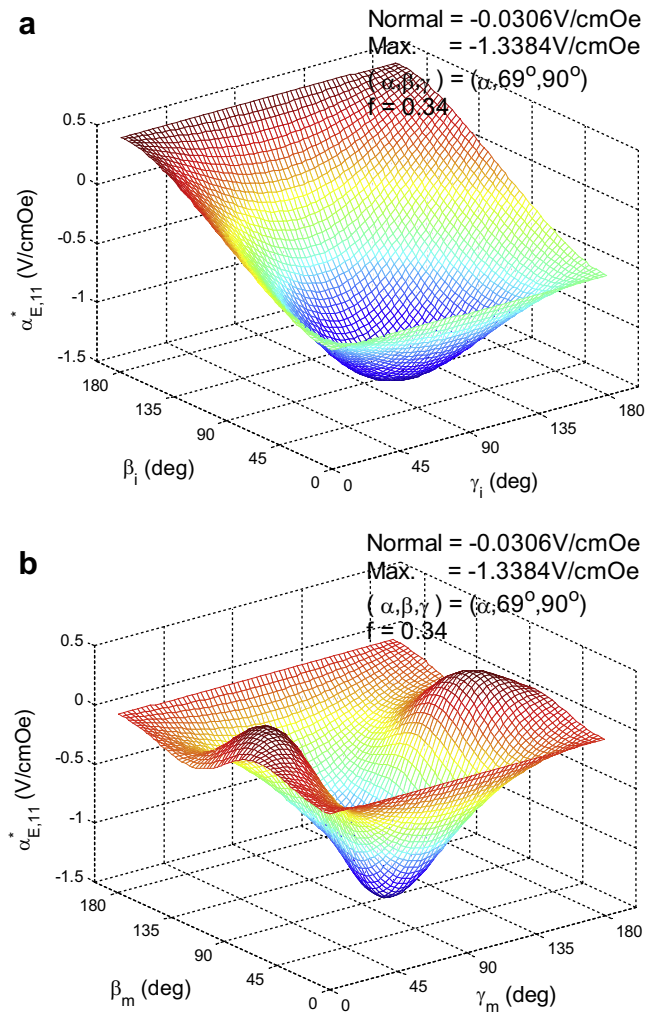

Fig. 8. The in-plane ME voltage coefficient of the BTO fibers in a CFO matrix for various orientations of BTO and CFO. The optimized constant occurs at both phases poled along the same direction.

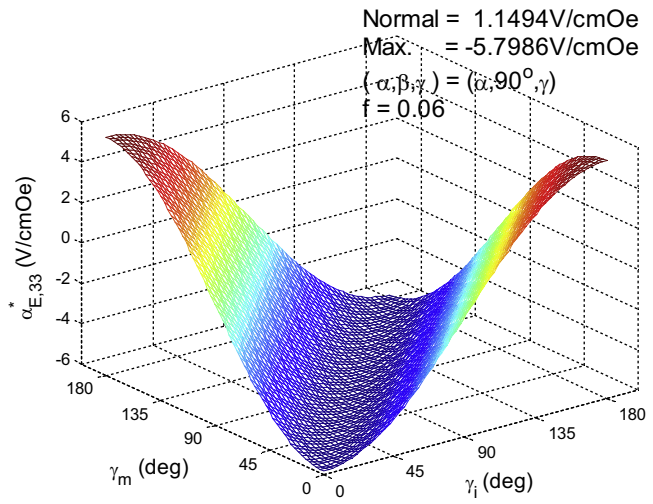

Fig. 9. The out-of-plane ME voltage coefficient of the BTO fibers in a CFO matrix for various orientations of BTO and CFO. The optimized constant occurs at both phases poled along the same direction.

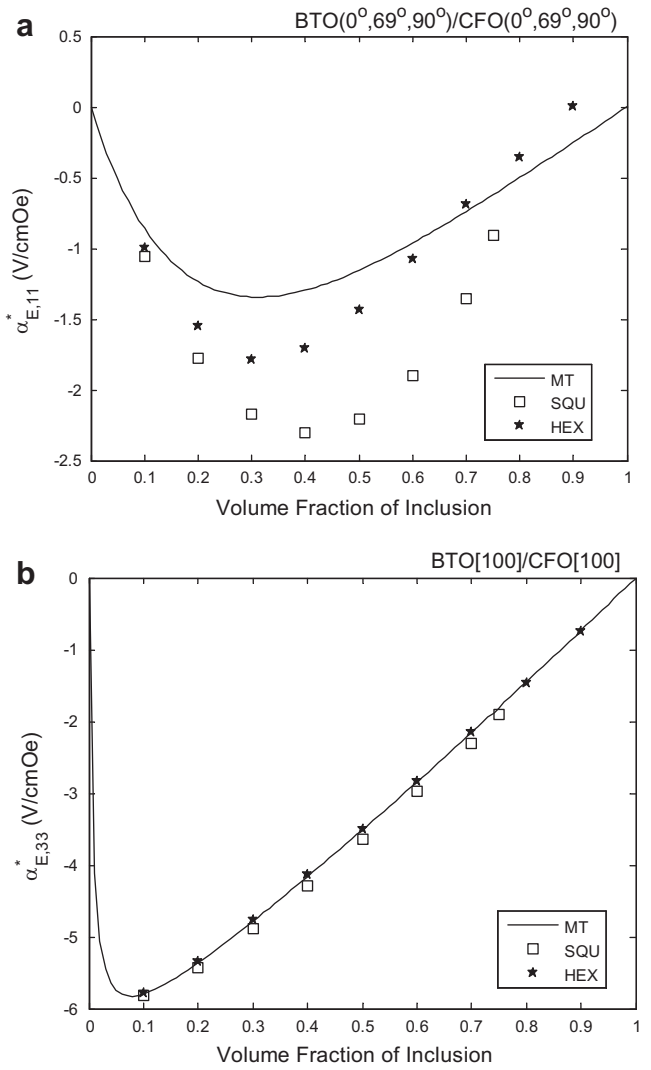

Fig. 10. The optimal ME voltage coefficients of the BTO fibers in a CFO matrix for various fiber volume fraction. (a) In-plane ME voltage coefficient $\alpha^*_{E,11}$. (b) Out-of-plane ME voltage coefficient $\alpha^*_{E,33}$.

$$
\begin{aligned}
U_M(d,x_2,x_3) &= U_M(-d,x_2,x_3) + \langle U_{M,1}\rangle 2d,\\
U_M\left(x_1,\sqrt{3}d,x_3\right) &= U_M\left(x_1,-\sqrt{3}d,x_3\right) + \langle U_{M,2}\rangle 2\sqrt{3}d,\\
U_M(x_1,x_2,d) &= U_M(x_1,x_2,-d) + \langle U_{M,3}\rangle 2d.
\end{aligned}
\tag{16}
$$

In order to determine the effective properties of the multiferroic composite, the strain, electric field, and magnetic field states are applied individually to the unit cell. The boundary conditions have to be applied to the unit cell in such a way that, apart from one component of the strain, electric field, or magnetic field $\langle U_{M,i}\rangle$ in Eq. (15) for square arrays or (16) for hexagonal arrays, all other components are made equal to zero. Then each effective coefficient can be determined by (9). We perform the finite element analysis using the software COMSOL Multiphysics.

3. Numerical results and optimization

We consider two systems of interest. For the piezoelectric material, we choose the widely used $BaTiO_3$ ceramic, while we choose $CoFe_2O_4$ as the piezomagnetic phase which has been studied by other researchers. Both of them are with 6 mm symmetry. We consider square and hexagonal arrays in finite element analysis, and both cases, i.e., both CFO fibers in a BTO matrix and BTO fibers in a CFO matrix. The independent material constants of these constituents are given in Table 1 in Voigt notation, where the x_1x_2 plane is isotropic and the poling direction/magnetic axis is along the x_3-direction.

In our study, we are particularly interested in the effective magnetoelectric (ME) response. The induced voltage is proportional to the applied magnetic field and the constant of proportionality is the effective ME voltage coefficient. It

combines the coupling and dielectric coefficients, and is defined by

$$\alpha^*_{E,ij} = \lambda^*_{ij}/\kappa^*_{ij}, \tag{17}$$

where there is no summation for the repeated indices. We seek to optimize this ME voltage coefficient with respect to the crystallographic orientation of the materials. Specifically we consider the in-plane ($\alpha^*_{E,11}$) and out-of-plane ($\alpha^*_{E,33}$) coupling constants. However, this is a highly nonlinear problem, therefore we resort to a brute-force approach where we create a fine grid of Euler angles and exhaustively compare the values on this grid.

3.1. Piezomagnetic fibers in a piezoelectric matrix

To check the correctness of our model, we first perform a numerical computation for CFO fibers in a BTO matrix with 6 mm material symmetry about the fiber axis. Fig. 3 shows the ME voltage coefficients for this composite. The finite element analysis is estimated for discrete volume fractions and stops around $f = \pi/4$ and $f = \pi/2\sqrt{3}$ for the square and hexagonal arrays, respectively, when the inclusions touch. The prediction of the Mori-Tanaka's approach is in good agreement with the result of the finite element analysis. The maximum ME voltage coefficient $\alpha^*_{E,11}$ is -0.0244 V/cmOe at volume fraction $f = 0.98$, while the maximum $\alpha^*_{E,33} = 1.2288$ V/cmOe at volume fraction $f = 0.94$. Note that the results of the hexagonal array are closer to the Mori–Tanaka's estimation than those of the square array. This is because a hexagonal array is a closed packing structure, and the Mori–Tanaka's model allows the inclusion to fulfill the matrix. In addition a square array lacks the transversely isotropy that this composite possesses (Li, 2000b).

We now turn to the optimization of this composite. For each orientation, we follow the procedure developed in

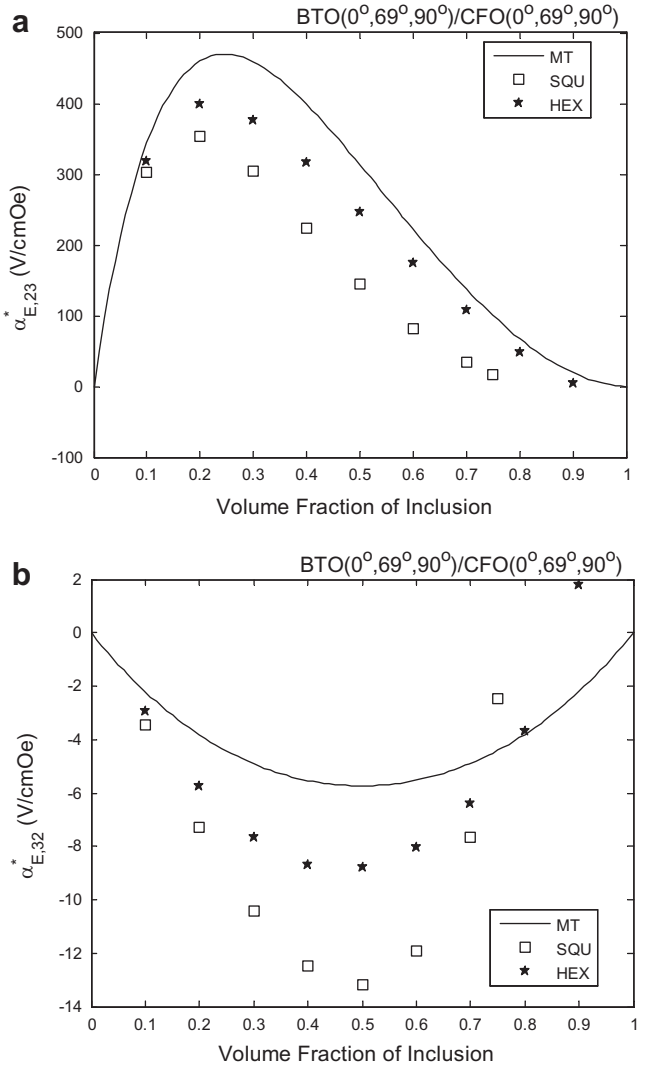

Fig. 11. The off-diagonal ME voltage coefficients of the BTO fibers in a CFO matrix for various fiber volume fraction. (a) ME voltage coefficient $\alpha^*_{E,23}$. (b) ME voltage coefficient $\alpha^*_{E,32}$.

Section 2 to obtain the magnetoelectric voltage coefficient. The reference volume fraction is $f = 0.98$ for calculating optimal $\alpha^*_{E,11}$, while it is chosen as 0.94 when calculating optimal $\alpha^*_{E,33}$ since these happen to be optimal at the normal cut. The orientation of both materials are arbitrary.

Fig. 4 shows the ME voltage coefficient $\alpha^*_{E,11}$ with respect to the crystallographic orientation of CFO and BTO. It happens to be optimal when the poling direction of piezoelectric phase coincides with the magnetic axis of the piezomagnetic phase. We observe that the maximum of -2.4823 V/cmOe occurs at Euler angles $(\alpha, \beta, \gamma) = (\alpha, 90^\circ, 90^\circ)$, where α is arbitrary. This degeneracy of optimal orientation reflects the 6 mm symmetry. Further, if $\alpha = 0$, it is equivalent to the poling direction/magnetic axis along [010]. Significantly, the optimized value of -2.4823 V/cmOe is almost *one hundred and one* times higher than -0.0244 V/cmOe, which is the value of the normal cut where the *c* axis of the CFO and BTO is along the fiber axis.

We show how the ME voltage coefficient $\alpha^*_{E,33}$ depends on its orientation in Fig. 5. The maximum value is -6.2079 V/cmOe at the optimal orientation $(\alpha, \beta, \gamma) = (\alpha, 90^\circ, \gamma)$ of both phases, and this is as much as *five* times higher than the value of 1.2288 V/cmOe at the normal cut.

Fig. 6 shows the effect of volume fraction f on the ME voltage coefficients. The piezoelectric phase is poled along one of the optimized directions, say $(\alpha, \beta, \gamma) = (0, 90^\circ, 90^\circ)$ or equivalently [010], and the piezomagnetic phase is along the same optimized magnetic axis. The maximum value is obtained at piezoelectric material almost vanish at volume fraction $f = 0.98$ and 0.92 for ME voltage coefficient $\alpha^*_{E,11}$ and $\alpha^*_{E,33}$, respectively. The maximum value of $\alpha^*_{E,11}$ is -2.4823 V/cmOe while that of $\alpha^*_{E,33}$ is -6.2357 V/cmOe both of these evaluated at their optimal orientations.

3.2. Piezoelectric fibers in a piezomagnetic matrix

We now turn to the composite made of BTO fibers in a CFO matrix. Similarly, we begin with the case of the material symmetry about the fiber axis, i.e. along [001]. The maximum $\alpha^*_{E,11}$ is -0.0306 V/cmOe at $f = 0.34$ and $\alpha^*_{E,33}$ is 1.1494 V/cmOe at $f = 0.06$ at their normal orientation (Fig. 7).

Figs. 8 and 9 show the magnetoelectric voltage coefficient $\alpha^*_{E,11}$ and $\alpha^*_{E,33}$ as a function of orientation for the case where the volume fraction is corresponding to their optimal value at the normal cut. We find that the maximum coupling coefficient is -1.3384 V/cmOe with $(\alpha, \beta, \gamma) = (\alpha, 69^\circ, 90^\circ)$ or $(\alpha, 111^\circ, 90^\circ)$ for $\alpha^*_{E,11}$. The plot for $(\alpha, 111^\circ, 90^\circ)$ is similar to Fig. 8 but with 180° reverse with respect to β. For $\alpha^*_{E,33}$, the maximum value is -5.7986 V/cmOe with $(\alpha, 90^\circ, \gamma)$. If we choose $\alpha = 0$ and $\gamma = 0$, the optimized direction is equivalent to [100].

Fig. 10 shows the effect of fibrous volume fraction on the ME voltage coefficients. For the optimized volume fraction, the numbers are -1.3441 V/cmOe and -5.8250 V/cmOe ($f = 0.08$), respectively. All of these are evaluated at their respective optimal orientation. Note that although the difference between the results of finite element analysis and Mori–Tanaka's method is larger in Fig. 10(a), the trend is similar for both methods. One reason of the deviation is that because the ME voltage coefficient is an indirect calculated value through Eq. (17). The effective permittivity κ^*_{11} approaches to zero hence is sensitive when calculating $\alpha^*_{E,11}$. Further, the magnetoelectric coefficient λ^*_{11} of this case has larger difference between the two approaches.

Finally, we observe that there are off-diagonal elements of $\alpha^*_{E,23}$ and $\alpha^*_{E,32}$ when the poling direction/magnetic axis is at the orientation $(\alpha, \beta, \gamma) = (\alpha, 69^\circ, 90^\circ)$. Fig. 11 shows how these coefficients depend on the volume fraction. Remarkably, the maximum $\alpha^*_{E,23}$ is 469.6768 V/cmOe ($f = 0.25$), while that of $\alpha^*_{E,32}$ is -5.7340 V/cmOe ($f = 0.50$).

4. Concluding remarks

In this work, we have proposed a theoretical framework to compute the effective magnetoelectric response of a piezoelectric–piezomagnetic fibrous composite. We have used it to show that, for anisotropic materials as in single crystals, the optimal ME response is obtained for non-trivial orientations. For the CFO fibers in a BTO matrix, the highest in-plane magnetoelectric voltage coefficient $\alpha^*_{E,11}$ at its optimized crystallographic orientation is 2.4823 V/cmOe, which is 101 times larger than that of a fibrous composite made with the normal cut type CFO and BTO single crystals. The out-of-plane ME voltage coefficient, $\alpha^*_{E,33}$, on the other hand, can be increased around five times to 6.2079 V/cmOe. For the BTO fibers in a CFO matrix, the in-plane and out-of plane ME voltage coefficients can be increased around 43 times and 5 times respectively compared to the normal orientation. The dependence of the magnetoelectric voltage coefficient with respect to the volume fraction f was also determined when both phases poled along the optimized direction. The coefficients varied with the volume fraction and were optimized when the piezoelectric phase approaches zero for the case of CFO fibers in a BTO matrix. Finally, the results are compared to finite element analysis and show good agreement.

Acknowledgement

We gratefully acknowledge Professor J. Y. Li for the Fortran code of Eshelby tensor. We are grateful to the financial support of National Science Council, Taiwan, under Contract No. NSC 100-2628-E-009-022-MY2.

References

Aboudi, J., 2001. Micromechanical analysis of fully coupled electro-magneto-thermo-elastic multiphase composites. Smart Mater. Struct. 10, 867–877.

Alshits, V.I., Darinskii, A.N., Lothe, J., 1992. On the existence of surface waves in half-infnite anisotropic elastic media with piezoelectric and piezomagnetic properties. Wave Motions 16, 265–284.

Arfken, G.B., Weber, H.J., 2001. Mathematical Methods for Physicists. Academic Press, San Diago, pp. 199.

Astrov, D.N., 1960. The magnetoelectric effect in antiferromagnetics. Sov. Phys. JETP 11, 708–709.

Benveniste, Y., 1995. Magnetoelectric effect in fibrous composites with piezoelectric and piezomagnetic phases. Phys. Rev. B 51, 16424–16427.

Bichurin, M.I., Petrov, V.M., Srinivasan, G., 2003. Theory of low-frequency magnetoelectric coupling in magnetostrictive-piezoelectric bilayers. Phys. Rev. B 68, 054402.

Camacho-Montes, H., Sabina, F.J., Bravo-Castillero, J., Guinovart-Díaz, R., Rodríguez-Ramos, R., 2009. Magnetoelectric coupling and cross-

property connections in a square array of a binary composite. Int. J. Eng. Sci. 47, 294–312.
Eerenstein, W., Mathur, N.D., Scott, J.F., 2006. Multiferroic and magnetoelectric materials. Nature 442, 759–765.
Fiebig, M., 2005. Revival of the magnetoelectric effect. J. Phys. D: Appl. Phys. 38, R123–R152.
Huang, J.H., Kuo, W.-S., 1997. The analysis of piezoelectric/piezomagnetic composite materials containing ellipsoidal inclusions. J. Appl. Phys. 81, 1378–1386.
Kittel, C., 2005. Introduction to Solid State Physics. John Wiley & Sons, New Jersey, p.8.
Kuo, H.-Y., 2011. Multicoated elliptic fibrous composites of piezoelectric and piezomagnetic phases. Int. J. Eng. Sci. 49, 561–575.
Kuo, H.-Y., Pan, E., 2011. Effective magnetoelectric effect in multicoated circular fibrous multiferroic composites. J. Appl. Phys. 109, 104901.
Kuo, H.-Y., Slinger, A., Bhattacharya, K., 2010. Optimization of magnetoelectricity in piezoelectric–magnetostrictive bilayers. Smart Mater. Struct. 19, 125010.
Lee, J., Boyd IV, J.G., Lagoudas, D.C., 2005. Effective properties of three-phase electro-magneto-elastic composites. Int. J. Eng. Sci. 43, 790–825.
Li, J.Y., 2000a. Magnetoelectroelastic multi-inclusion and inhomogeneity problems and their applications in composite materials. Int. J. Eng. Sci. 38, 1993–2001.
Li, S., 2000b. General unit cells for micromechanical analyses of unidirectional composites. Composites: Part A 32, 815–826.
Li, J.Y., Dunn, M.L., 1998a. Micromechanics of magnetoelectroelastic composite materials: average fields and effective behaviour. J. Intel. Mat. Syst. Struct. 9, 404–416.
Li, J.Y., Dunn, M.L., 1998b. Anisotropic coupled-field inclusion and inhomogeneity problems. Philos. Mag. A 77, 1341–1350.
Liu, G., Nan, C.-W., Cai, N., Lin, Y., 2004. Calculations of giant magnetoelectric effect in multiferroic composites of rare-earth-iron alloys and PZT by finite element method. Int. J. Solids Struct. 41, 4423–4434.
Nan, C.-W., 1994. Magnetoelectric effect in composites of piezoelectric and piezomagnetic phases. Phys. Rev. B 50, 6082–6088.
Nan, C.-W., Bichurin, M.I., Dong, S., Viehland, D., Srinivasan, G., 2008. Multiferroic magnetoelectric composites: historical perspective, status, and future directions. J. Appl. Phys. 103, 031101.
Nye, J.F., 1985. Physical Properties of Crystals. Oxford University Press, Oxford.
Rado, G.T., Folen, V.J., 1961. Observation of the magnetically induced magnetoelectric effect and evidence for antiferromagnetic domains. Phys. Rev. Lett. 7, 310–311.
Srinivas, G., Rasmussen, E.T., Galleogos, J., Srinivasan, R., Bokhan, Y.I., Laletin, V.M., 2001. Magnetoelectric bilayer and multilayer structures of magnetostrictive and piezoelectric oxides. Phys. Rev. B 64, 214408.
Srinivas, S., Li, J.Y., Zhou, Y.C., Soh, A.K., 2006. The effective magnetoelectroelastic moduli of matrix-based multiferroic composites. J. Appl. Phys. 99, 043905.
Wang, Y., Or, S.W., Chan, H.L.W., Zhao, X., Luo, H., 2008. Enhanced magnetoelectric effect in longitudinal-transverse mode Terfenol-D/$Pb(Mg_{1/3}Nb_{2/3})O_3$-$PbTiO_3$ laminate composites with optimal crystal cut. J. Appl. Phys. 103, 124511.
Wu, T.-L., Huang, J.-H., 2000. Closed-form solutions for the magnetoelectric coupling coefficients in fibrous composites with piezoelectric and piezomagnetic phases. Int. J. Solids Struct. 37, 2981–3009.
Yang, P., Zhao, K., Yin, Y., Wan, H.G., Shu, J.S., 2006. Magnetoelectric effect in magnetostrictive/piezoelectric laminate composite Terfenol-D/$LiNbO_3$[(zxtw)129°/30°]. Appl. Phys. Lett. 88, 172903.